JACS
JOURNAL OF THE AMERICAN CHEMICAL SOCIETY
pubs.acs.org/JACS
Article

Conformation, and Charge Tunneling through Molecules in SAMs

Lee Belding,[§] Samuel E. Root,[§] Yuan Li, Junwoo Park, Mostafa Baghbanzadeh, Edwin Rojas, Priscilla F. Pieters, Hyo Jae Yoon, and George M. Whitesides*

Cite This: J. Am. Chem. Soc. 2021, 143, 3481−3493
Read Online
ACCESS | Metrics & More | Article Recommendations | Supporting Information

ABSTRACT: This paper demonstrates that the molecular conformation (in addition to the composition and structure) of molecules making up self-assembled monolayers (SAMs) influences the rates of charge tunneling (CT) through them, in molecular junctions of the form $Au^{TS}/S(CH_2)_2CONR^1R^2//Ga_2O_3/EGaIn$, where R^1 and R^2 are alkyl chains of different length. The lengths of chains R^1 and R^2 were selected to influence the conformations and conformational homogeneity of the molecules in the monolayer. The conformations of the molecules influence the thickness of the monolayer (i.e. tunneling barrier width) and their rectification ratios at ±1.0 V. When R^1 = H, the molecules are well ordered and exist predominantly in *trans*-extended conformations. When R^1 is an alkyl group (e.g., $R^1 \neq H$), however, their conformations can no longer be all-*trans*-extended, and the molecules adopt more *gauche* dihedral angles. This change in the type of conformation decreases the conformational order and influences the rates of tunneling. When $R^1 = R^2$, the rates of CT decrease (up to 6.3×), relative to rates of CT observed through SAMs having the same total chain lengths, or thicknesses, when R^1 = H. When $R^1 \neq H \neq R^2$, there is a weaker correlation (relative to that when R^1 = H or $R^1 = R^2$) between current density and chain length or monolayer thickness, and in some cases the rates of CT through SAMs made from molecules with different R^2 groups are different, even when the thicknesses of the SAMs (as determined by XPS) are the same. These results indicate that the thickness of a monolayer composed of insulating, amide-containing alkanethiols does not solely determine the rate of CT, and rates of charge tunneling are influenced by the conformation of the molecules making up the junction.

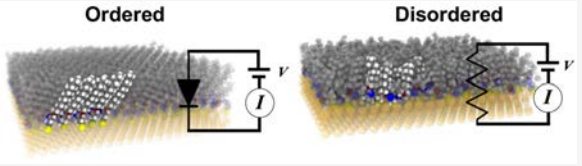

INTRODUCTION

When electrical charge tunnels through electrically insulating organic molecules between electrically conducting electrodes, the rate of tunneling follows (or is influenced by) the molecular and electronic structure of these molecules.[1] For junctions based on self-assembled monolayers (SAMs) of saturated organic groups, a relevant question is "is the *conformation* of the molecule important in determining the rate of charge tunneling through it, or is it simply the number of, and nature of, *bonds*—independent of their conformation—that matter?" If the former is correct, the conformation can be used to influence the pathway (and rate) of charge tunneling (CT). If it is *not* important, then the molecular structure influences tunneling by some mechanism (e.g., perturbation of the electric field within the tunneling barrier) and thus the structure, width, average height, and shape of this barrier are independent of molecular conformation. Here, we study the simplest form of this question: is the rate of CT from one electrode to a second different or the same though *trans* and *gauche* fragments of a polymethylene $(CH_2)_n$ chain with the same number of carbon atoms?

To address this question, we synthesized dialkyl disulfides having the general structure $(S\text{-}(CH_2)_2\text{-}CON(R_1)(R_2))_2$ (where R_1 is an alkyl chain and R_2 is an alkyl group or a hydrogen atom) and made SAMs of them by adsorption onto evaporated, template-stripped gold surfaces (Au^{TS}). Figure 1 illustrates the assumptions underlying this design (and research) in their simplest form. When the group R_1 on nitrogen is a hydrogen (R_1 = H, R_2 = *n*-alkyl), the organic molecules making up the SAM can condense to a relatively high surface density through intermolecular hydrogen bonds. When $R_1 = CH_3$ or larger alkyl chain, steric interactions prevent this condensation, the molecules in the SAM are more separated, and there is an opportunity (in fact, the requirement) for the larger chain to bend into structures that have *gauche* conformations in order to increase the density of packing of the organic layer. Thus, introducing larger R_2 groups also introduces *gauche* conformations. This simple argument—without defining the details of these conformations—is the immediate justification of the paper. Molecular dynamics (MD) simulations reinforced our initial assumptions that (i) secondary amides have well-ordered, *trans*-extended geometries, (ii) symmetrical tertiary amides form SAMs that are not fully *trans* extended, and (iii) the unsymmetrical tertiary amides form SAMs with more disordered conforma-

Received: December 2, 2020
Published: February 23, 2021

https://dx.doi.org/10.1021/jacs.0c12571
J. Am. Chem. Soc. 2021, 143, 3481−3493

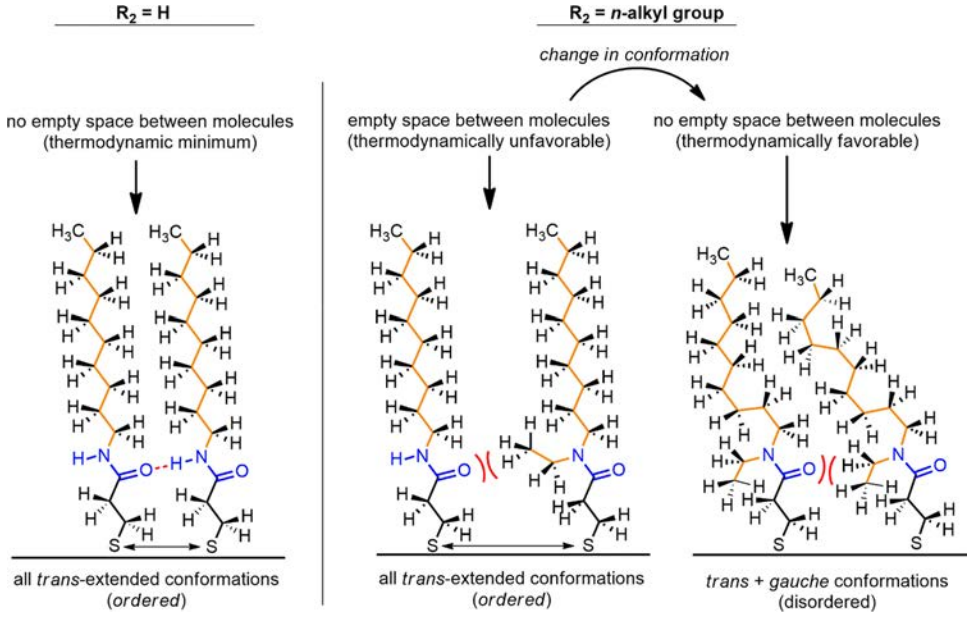

Figure 1. SAMs having the general structure S-$(CH_2)_2$-CON$(R_1)(R_2)$ (where R_1 is an alkyl chain and R_2 is an alkyl group or a hydrogen atom). When R_2 = H, adjacent amide groups can undergo hydrogen bonding and the molecules can adopt uniformly *trans* extended conformations. These ordered conformations allow the molecules in the SAM to fall into van der Waals contact and to pack close together, thus creating a more densely packed SAM. When R_2 = *n*-alkyl, the amide groups can no longer accommodate hydrogen bonding, and steric repulsion forces a larger distance between adjacent molecules, thus decreasing the packing density within the SAM. To avoid empty space, the alkyl chains R_1 and R_2 adopt a mixture of *gauche* and *trans* conformations.[2−4]

tions in comparison to secondary amides or symmetrical tertiary amides.

The question of how the molecular conformation affects tunneling is important for the ability to design or rationalize phenomena in at least three areas. (i) *Molecular electronics*: The transfer of charge by tunneling becomes more important in modern technology as electronic components approach the molecular scale[5−7] (for example, in capacitors, where organic monolayers have been explored to decrease leakage currents and thus reduce power consumption in complementary logic circuits based on organic field effect transistors[8,9]). (ii) *Biochemistry*: Charge tunneling is integral to the function of a number of important biological systems such as redox systems (both single-enzyme and membrane-embedded, multienzyme redox systems), DNA repair enzymes, and enzymes of nitrogen fixation.[10−15] (iii) *Theory*: The question of the relationship between HOMOs and LUMOs (both are important to tunneling) and the conformations of organic molecules (as opposed to their composition and structure) have been studied only briefly.[16,17]

The conformation of molecules may also be important in other areas, such as the activity of photocatalysts,[18] an understanding of the properties (and mechanism) of charge-transfer-based fluorophores,[19,20] charge transfer at an electrode/electrolyte interface,[21] and the development of corrosion inhibitors.[22] Here, a comparison of the rates of CT through organic molecules of similar structures but different conformations suggests that CT *is* influenced by the conformation of the molecule(s).

Self-assembled monolayers (SAMs) are model systems used (*inter alia*) to study charge transport through organic molecules[23−26] for the following reasons. (i) SAMs formed from *n*-alkanethiols have been extensively studied, have well-characterized, *trans*-extended conformations, and are ordered. (ii) Organic thiols of a wide range of structures are readily available and thus enable studies correlating the structure with the rates of tunneling. (iii) SAMs (as opposed to single molecules or a solution) are among the plausible physical systems with which to fabricate molecular electronic devices.[27]

Efforts to control charge tunneling through SAMs have focused on the electronic structure of the molecules: the nature of the molecule−metal contact,[28,29] conjugation,[30−32] dipole moments,[33,34] donor and acceptor systems,[35] and asymmetrically positioned chromophores.[36−38] The conformations of the molecules making up a SAM—rather than simply their bond connectivity—might also influence the rates of charge transport, by allowing longer-range orbital overlaps, by influencing the electronic structure, by changing the width, mean height, or energetic topography of the tunneling barrier, or by influencing intermolecular electronic interactions in the SAM. By a comparison of the thicknesses, surface coverages, rates of charge tunneling, and rectification ratios between well-ordered SAMs and structurally disordered SAMs (Figure 2), in this paper, we infer that the conformation *does* influence tunneling and that shorter distances between electrodes do not always imply larger tunneling rates (even in simple aliphatic molecules). We synthesized four series of dialkyl disulfides containing one amide group (Figure 2) having the general structure $(S\text{-}(CH_2)_2\text{-}CON(R_1)(R_2))_2$ (where R_1 is an alkyl chain and R_2 is an alkyl group or a hydrogen atom) and made SAMs of them by adsorption onto evaporated, template-stripped gold surfaces (Au^{TS}).[39]

The assumptions underlying this design (and research) is that molecules with secondary amides can adopt linear (*trans*-extended) conformations, but molecules with tertiary amides must adopt geometries that deviate from linearity by incorporating *gauche* conformations.

In tertiary amides (we supposed) larger differences between the lengths of the chain R_1 and R_2 would cause the molecules in the SAM to adopt conformations that were increasingly

https://dx.doi.org/10.1021/jacs.0c12571
J. Am. Chem. Soc. 2021, 143, 3481−3493

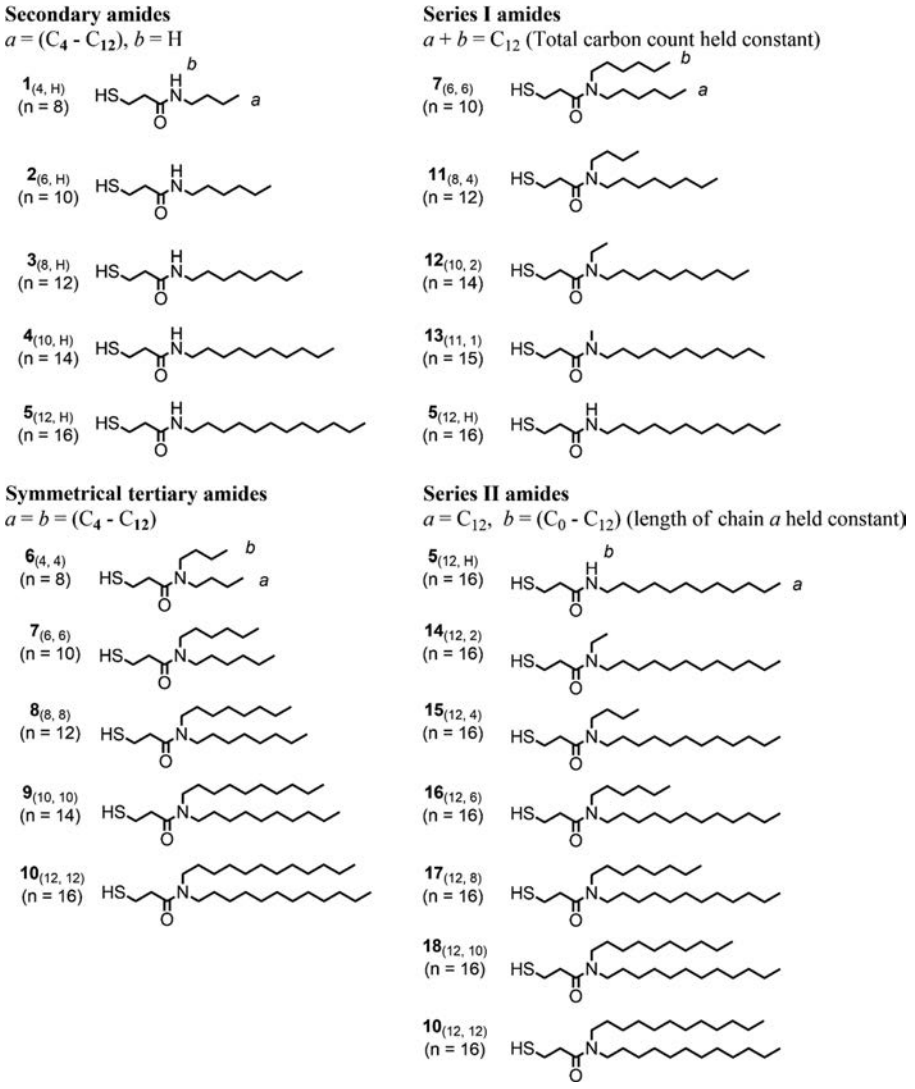

Figure 2. Structures of the *secondary amides* **1**−**5**, with the total number of atoms in the chain (n) ranging from 8 to 16. Structures of the *symmetrical tertiary amides*, **6**−**10**, where the length of chains a and b are the same. Structures of the *series I amides*: **5** and **7**−**13**, where the total number of carbon atoms in chain a and b is 12. Structures of the *series II amides*: **5**, **10**, and **14**−**18**, where the length of chain a is kept at 12 carbons, while the length of chain b is varied.

more disordered. If the two branching chains R_1 and R_2 have unequal lengths, they cannot both be linearly extended and maintain a uniform density in the SAM; there must be a change in conformation to eliminate void space in the SAM. The objective of this work was to determine if disordered conformations and ordered conformations of homologous molecules differed significantly in the rates of tunneling through them at a common voltage (+0.5 V).

We chose to use 3-mercaptopropionamides ($S\text{-}(CH_2)_2\text{-}CON\text{-}R_1R_2$; Figures 1 and 2) to synthesize conformationally ordered and disordered SAMs, because (i) they are synthetically simple to prepare, (ii) the amide nitrogen can be monoalkylated to form linear structures or dialkylated to form branched structures, (iii) the short anchoring group permits a large range of R_1 and R_2 (i.e. lengths of chains a and b), and (iv) our previous work has shown that molecules with amide groups in this position exhibit rectification of tunneling current and that this rectification is sensitive to the conformational order within the SAMs.[34]

For the molecules with the form $S\text{-}(CH_2)_2\text{-}CON(R_1)(R_2)$, we use the abbreviation $\mathbf{X}_{(a,b)}$, where **X** is the index number assigned to each molecule in this study, "a" is the number of carbon atoms in chain R_1, and "b" is the number of carbon atoms in R_2 (Figure 2). We also use n to represent the number of atoms making up the longest path in the molecules, including the $\text{-}(CH_2)_2\text{-}CON-$ anchoring group. The R_1 group (of length a) is an n-alkyl chain, and the R_2 substituent (of length b) is either an n-alkyl chain or a hydrogen atom.

We used a combination of molecular dynamics (MD) simulations and X-ray photoelectron spectroscopy (XPS) to characterize the thicknesses, surface coverages, and degrees of disorder within the SAMs. We ran all tunneling measurements using the EGaIn junction at a maximum applied bias of ±1.0 V. Amide-containing alkanethiols rectify current at 1.0 V and not at 0.5 V; therefore, we compare the rates of tunneling at +0.5 V and the rectification ratios at ±1.0 V. We define the rectification ratio (r) as the absolute value of the larger current density divided by the absolute value of the lower current density and include an indication of polarity: $r^+ = |J(+V)|/|J(-V)|$ or $r^- = |J(-V)|/|J(+V)|$. In this definition r is always ≥1. We note here—in our sign convention—that at positive bias (+V) the EGaIn electrode is oxidizing relative to

https://dx.doi.org/10.1021/jacs.0c12571
J. Am. Chem. Soc. 2021, 143, 3481−3493

the Au electrode and at negative bias (−V) the EGaIn electrode is reducing relative to the Au electrode.[36]

BACKGROUND

Liquid-like and Crystalline SAMs. SAMs made from *n*-alkanethiols exhibit length-dependent physical properties. For example, relative to SAMs with shorter (n < 12) chain lengths, those with longer chain lengths have larger water contact angles[4] and are more prone to leakage currents.[40−42]

Alkanethiol-based SAMs have four states (or phases), based on their chain length.[4] Below C_{10} (an *n*-alkanethiol SAM with 10 carbon atoms), SAMs exist in a "liquid-like" state, where the entropic free energy associated with vibrational, translational, and rotational motion is larger than the enthalpic free energy associated with intermolecular van der Waals interactions.[4] This liquid-like regime is associated with less conformational order and more *gauche* defects in comparison to those observed for SAMs with higher chain lengths.[4] Between $C_{9/10}$ and C_{14}, there is a transition from liquid-like to crystalline-like SAMs—a "wax-like" state—with physical properties between those of shorter and longer chain lengths. At or above C_{14}, the alkanethiols are well-ordered and form rigid, crystalline SAMs that have all-*trans* conformations.[4,43] Such length-dependent thermophysical transitions also occur with SAMs of linear alkyl phosphonates on aluminum oxide: junctions formed with top electrodes of thermally evaporated gold[41] and droplets of mercury[42] both exhibited increased current density for longer chains (n > 12) than would have been expected on the basis of thickness considerations alone. These reductions in the attenuation of current (i.e., leakage currents) were attributed to the presence of voids and thickness inhomogeneities at grain boundaries.

Amide-Containing SAMs. Previous studies have concluded that SAMs made from alkanethiols containing secondary amides ($HS(CH_2)_nCONHR$) form well-ordered monolayers with strong intermolecular hydrogen bonding between neighboring amide groups throughout the backbone.[44−48] SAMs made from amide-containing alkanethiols, like those made from simple alkanethiols, become more crystalline with increasing chain length.[49,50] The different physical states of amide-containing SAMs, however, occur at different chain lengths ($n \approx 10-12$) in comparison to *n*-alkanethiols ($n \approx 12-14$) and depend on the position of the amide group in the molecule.[49,50]

Influence of Branching Chains on the Physical Properties of SAMs. Spectroscopic and microscopic surface characterization by Lee et al.[51−53] and the study of spiroalkanedithiols (2,2-dialkylpropanedithiols) by Carmichael et al.,[54] using bis-substituted phosphinic acids, and by us,[55] using dialkyl sulfides, have shown that SAMs made from molecules that have two alkyl chains of equal length, diverging from a single anchoring group (symmetrical branching), form densely packed, well-ordered SAMs, while those made from molecules with two alkyl chains of unequal length (asymmetrical branching) form densely packed but disordered SAMs.

Pathway of Charge Tunneling through SAMs. Early work on charge transport through small, nonaromatic, organic molecules (e.g. alkanethiols,[56,57] thiol-terminated norbornylogs[58,59]) largely agreed on a mechanism for tunneling that was "through-bond", in which charge tunnels through the σ-orbital framework (that is, largely the chain of C−C bonds) of the molecules, with rates that depended on the dihedral angle of the bonds (favoring *trans* geometries).[60−63] More recent work, however, based primarily (but not entirely[64]) on experimental observations and theoretical models[65] of temperature-dependent tunneling rates[66−68]—which are interpreted as evidence of conformationally dependent (and thus thermally activated) tunneling—suggest that charge tunneling takes place, at least in part, via intramolecular[69−71] or intermolecular[71] through-space pathways.

The conformations of molecules within a SAM are influenced by—in addition to their chemical structures—the topography of the bottom electrode. Grain boundaries in the substrate are associated with "thin-area defects" because they cause localized disorder in the SAM.[40,72,73] It is generally assumed that thin-area defects lead to tunneling currents through molecular junctions that are higher than expected, given the chain lengths of the molecules, because the orientations of these molecules are disordered and leave a shorter distance between the bottom and top electrodes.[40−42] This rationale has been used to explain the observation that the rates of charge tunneling through SAMs made on template-stripped (TS) substrates (which have fewer exposed grain boundaries in comparison to substrates made from direct evaporation[72,73]) are lower than rates of tunneling through SAMs with the bottom electrodes made by direct evaporation.[72]

Rectification in SAMs Containing Amides. We have recently reported that SAMs with polar functional groups (amides, ureas, and thioureas) located close to a bottom Ag^{TS} electrode rectify current ($r^+ \approx 20$) at an applied bias of greater than ~0.6 V[34]—where tunneling takes place predominantly by a Fowler−Nordheim (F-N) mechanism. Rectification in these systems is related to the magnitude (and direction) of the net dipole moment perpendicular to (and away from) the bottom electrode.[74] Changing the orientation of the amide group (from −CONH− to −NHCO−) or disrupting the structure of the SAM (by *N*-methylation) eliminated rectification in these systems, presumably because these physical changes reduce the net dipole moment perpendicular to the bottom electrode.

EXPERIMENTAL DESIGN

We used secondary amides that form well-ordered SAMs (Figure 2) as a control group and introduced changes in the geometry and conformation of the molecules by using tertiary amides. Replacing the hydrogen atom in secondary amides with another alkyl chain prevents the molecules from adopting fully *trans* extended geometries and eliminates the potential for hydrogen bonding between adjacent amide groups in the SAM. This H-bonding helps order the conformations of secondary amides.[44]

We prepared three other series of amides, one that has two alkyl chains of equal length (symmetrical tertiary amides) and two that have alkyl chains with varying lengths, to dissect the competing effects of thickness and conformational disorder. The symmetrical tertiary amides were designed to introduce a deviation from linear (*trans*-extended) geometries while retaining the perpendicular orientation of the chain lengths. Series I and series II amides (Figure 2) were designed to cause the molecules in the SAM to adopt different conformations (and thus have a higher population of *gauche* bonds in comparison to the longer and better-ordered analogues). In series I amides, the total number of carbon atoms in both chains is constant, and in series II amides the length of the longest alkyl chain remained constant.

EXPERIMENTAL SECTION

We, and others, have described the electrical measurements using the EGaIn junction, which we include in the section S2 in the Supporting

https://dx.doi.org/10.1021/jacs.0c12571
J. Am. Chem. Soc. 2021, 143, 3481−3493

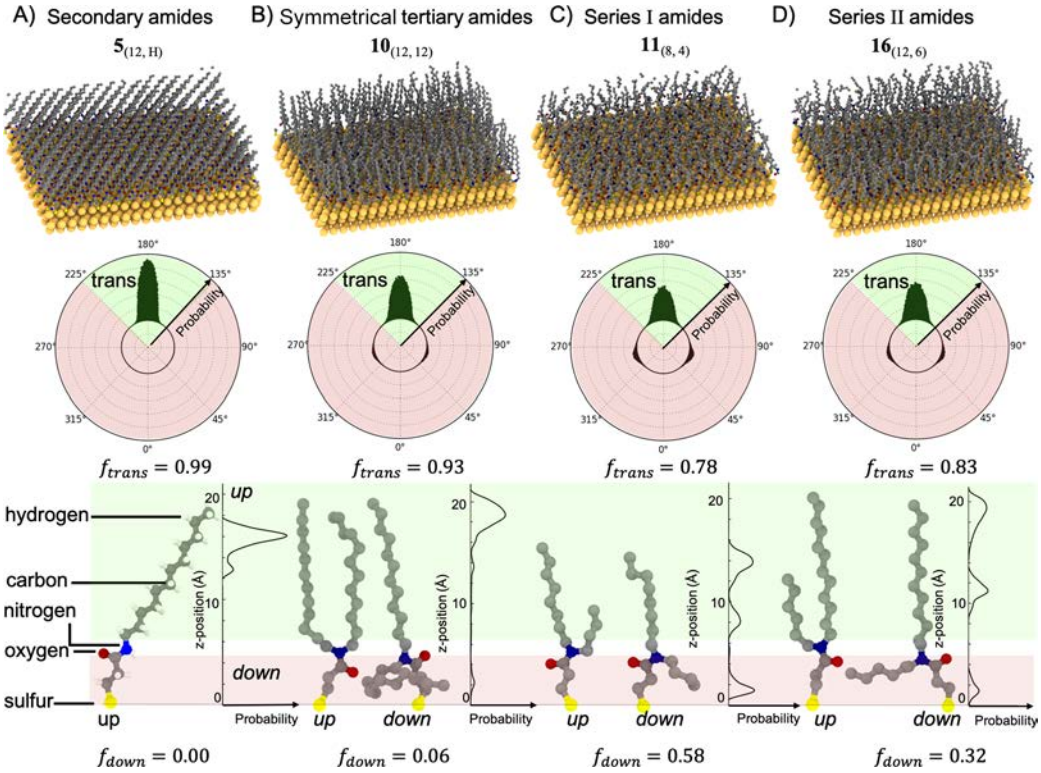

Figure 3. (top) Snapshots from the equilibrated MD simulation trajectories. (middle) Histograms from the MD simulations representing the probability density function obtained from all C−C−C−C dihedral angles within a simulated SAM, which are used to compute f_{trans}. (bottom) Selected, individual molecules from the MD simulations that depict branches pointing "up" and "down", alongside the probability density functions of the terminal methyl with respect to the z position, which are used to calculate f_{down}. Hydrogen atoms are excluded from the molecules for clarity. Elements are labeled according to color as indicated on the bottom left. Examples from (A) the secondary amide control group ($\mathbf{5}_{(12,H)}$), (B) the symmetrical tertiary amides ($\mathbf{10}_{(12,12)}$), (C) the series I amides ($\mathbf{11}_{(8,4)}$), and (D) the series II amides ($\mathbf{16}_{(12,6)}$).

Information. SAMs were prepared using standard published protocols (see section S3 in the Supporting Information). Section S11 in the Supporting Information also details the synthesis and characterization of all molecules and intermediates used for the formation of SAMs. It also includes characterization of the SAMs, including detailed procedures for angle-resolved X-ray photoelectron spectroscopy (ARXPS) (section S4 in the Supporting Information).

COMPUTATIONAL DETAILS

To characterize the thickness, packing, and conformational structure of the SAMs, we performed MD simulations with the OPLS-2005 force field[75] implemented in LAMMPS[76] and visualized with OVITO[77] (Figure 3). The complete computational methodology and details are summarized in section S5 in the Supporting Information.

From the equilibrated simulations, we define the height of each molecule in the monolayer as the vertical distance between the sulfur atom and the terminal hydrogen atom in the molecule with the maximum z position. We then approximated the thickness of the simulated monolayer by averaging the heights of all the molecules in the SAM over a duration of 5 ns and the roughness of the monolayer by using the standard deviation of the molecular height distribution (as indicated by the error bars in the plots).

We chose to compute two statistical metrics from the simulations to characterize the conformational disorder present in the SAM—both of which were calculated by taking ensemble averages over all of the molecules in the equilibrated SAM at 300 K over a duration of 5 ns: (1) the fraction of C−C−C−C dihedral angles in the *trans* orientation, f_{trans}, and (2) the fraction of chains that were not oriented normal to the surface, i.e. pointing down or to the side, f_{down} (Figure 3).

The fraction of C−C−C−C dihedral angles (θ) in the *trans* orientation was defined as

$$f_{trans} = \frac{N_{trans}}{N_{total}} \quad (1)$$

where N_{trans} is the average number of dihedral angles with θ ranging from 135° to 225° and N_{total} is the total number of dihedral angles. This cutoff was chosen on the basis of an inspection of the dihedral angle probability distributions shown in the middle of Figure 3A−D, to ensure that the entire peak associated with thermal fluctuations about the *trans*-orientation minimum energy state was included in the calculation. We also computed the N−C−C−C dihedral angle and included the data in the Supporting Information but found that the trends for the dihedral angles qualitatively match, and so for simplicity, we restrict our discussion to the C−C−C−C dihedral angle. Thus, f_{trans} does not account for any conformational disorder when a chain is one or two carbons in length (i.e. chain b in $\mathbf{12}_{(10,2)}$, $\mathbf{13}_{(11,1)}$, or $\mathbf{14}_{(12,2)}$), because there is no C−C−C−C dihedral angle. The states of C−N−C−C and the N−C−C-C dihedral angles (and the rest of the dihedral angles in the alkyl chain), however, couple cooperatively to determine whether the shorter alkyl chain in the branched molecule is oriented normal to the surface or pointing "down", as quantified by our alternative statistical metric f_{down}.

One observation from our simulations was that, in the conformationally disordered SAMs, there were a significant fraction of branched alkyl chains that were not oriented normal to the surface (Figure 3B−D, bottom). Specifically, we observed that the equilibrium probability distribution of the z position of the terminal methyl groups, $P(z)$, could contain a single peak (secondary amides), two peaks (symmetrical tertiary amides), or up to three peaks (series I and II amides). By integrating the areas of the respective peaks, we were able to calculate the fraction of chains pointed down, f_{down}, i.e.

https://dx.doi.org/10.1021/jacs.0c12571
J. Am. Chem. Soc. 2021, 143, 3481−3493

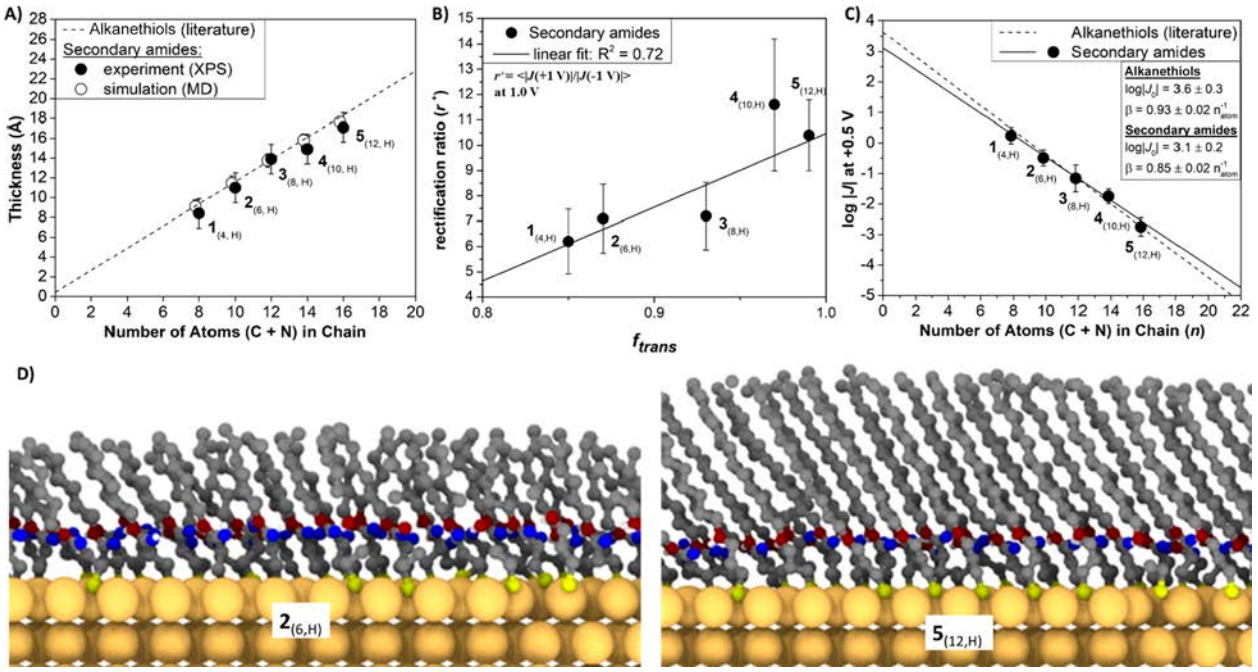

Figure 4. (A) Plot of the measured (filled circles) and simulated (empty circles) thicknesses of SAMs made from secondary amides **1** - **5**, as a function of their chain length. The dashed line represents the corresponding data (from the literature[80]) for alkanethiols. (B) Plot of rectification ratios (r^+) measured at 1.0 V as a function of the conformational order (defined by f_{trans}) of the SAM. (C) Tunneling rates measured for the secondary amides, as a function of their chain length, with the measured rates of alkanethiols[80] for comparison. (D) Selected snapshots from the MD simulations of SAMs **2** and **5** (1.5 nm cross sections), depicting their thickness and conformation. Hydrogen atoms have been removed for clarity.

with a terminal CH_3 group that was not at or near the farthest possible z position in the SAM for that particular alkyl chain

$$f_{\text{down}} = \int_0^{z^*} P(z)\,\mathrm{d}z \tag{2}$$

where z^* is a cutoff height, chosen by visual inspection, to include only the bottom peak in the probability distribution (Figure 3A–D, bottom). A similar limitation to f_{trans} exists for f_{down}: that is, for $\mathbf{13}_{(11,1)}$ the lone CH_3 group of chain *b*" will always have the same orientation/conformation.

RESULTS AND DISCUSSION

Thickness, Packing Density, and Conformation of SAMs Containing Amides. We expected the differences in structure among the molecules we studied to influence three related physical characteristics of the SAMs: *thickness of the monolayer*, *their packing density*, and *conformation of the molecules*. To determine the effect of conformation on charge tunneling, we must also understand the influence of thickness and packing density. Sections S4–7 in the Supporting Information contain details of our measurements of thickness and packing density by XPS and by MD simulations and a discussion of these techniques in the context of this work.

Thickness. For *n*-alkanethiols, the rate of charge tunneling correlates exponentially with the thickness of the SAM, according to the simplified Simmons equation $J(V) = J_0(V)\,e^{-\beta d}$ [33,78,79] where d is the thickness of the SAM. In this work, if the rate of tunneling correlates directly with the thickness of the SAM, even as the conformation of the molecules change, then charge tunneling is likely a "through-space" phenomenon that depends primarily on the distance between the two electrodes and the electrostatic field generated by the molecules making up the SAM. If, however, the rate of charge transport is not a direct function of monolayer thickness, we must conclude that changes in packing density and/or the conformations of the molecules in the SAM influence tunneling. In our discussions involving thickness, we refer to the *experimentally* determined thickness (as determined by ARXPS, as opposed to the thickness obtained from the MD simulations), unless specifically specified otherwise. We note here that the calculation of monolayer thickness (and packing density) from ARXPS experiments involves the assumption of a fixed inelastic mean free path of photoelectrons (section S4 in the Supporting Information), which is a rough approximation: the attenuation of photoelectrons is expected to be directly correlated with packing density.

Packing Density. The packing density of a monolayer is defined as the number of molecules m (in moles) per unit of surface area (m/cm^2). The tertiary amides used in this work result in structures that are branched (two alkyl chains for each sulfur anchoring group) and will thus have larger intermolecular distances within the monolayer in comparison to secondary amides or alkanethiols and should thus form SAMs with lower packing densities. If changes in packing density (i.e., number of molecules per area) determine the rate of tunneling by changing the number of electrical conduits, the rate of charge tunneling should scale linearly with packing density. That is, when only uniformly structured SAMs are considered, a SAM with a packing density of 0.5×10^{-9} mol/cm^2 should have half the number of conduits per unit area as a SAM with a packing density of 1.0×10^{-9} mol/cm^2. In this work, we use ARXPS (see section S4 in the Supporting Information for details) to measure the packing densities of SAMs and employ decanethiol (reported[23] on Au as 1.0×10^{-9} mol/cm^2) as a standard.

Conformation. We used the two disorder parameters from our MD simulations (described above in the Computational

https://dx.doi.org/10.1021/jacs.0c12571
J. Am. Chem. Soc. 2021, 143, 3481–3493

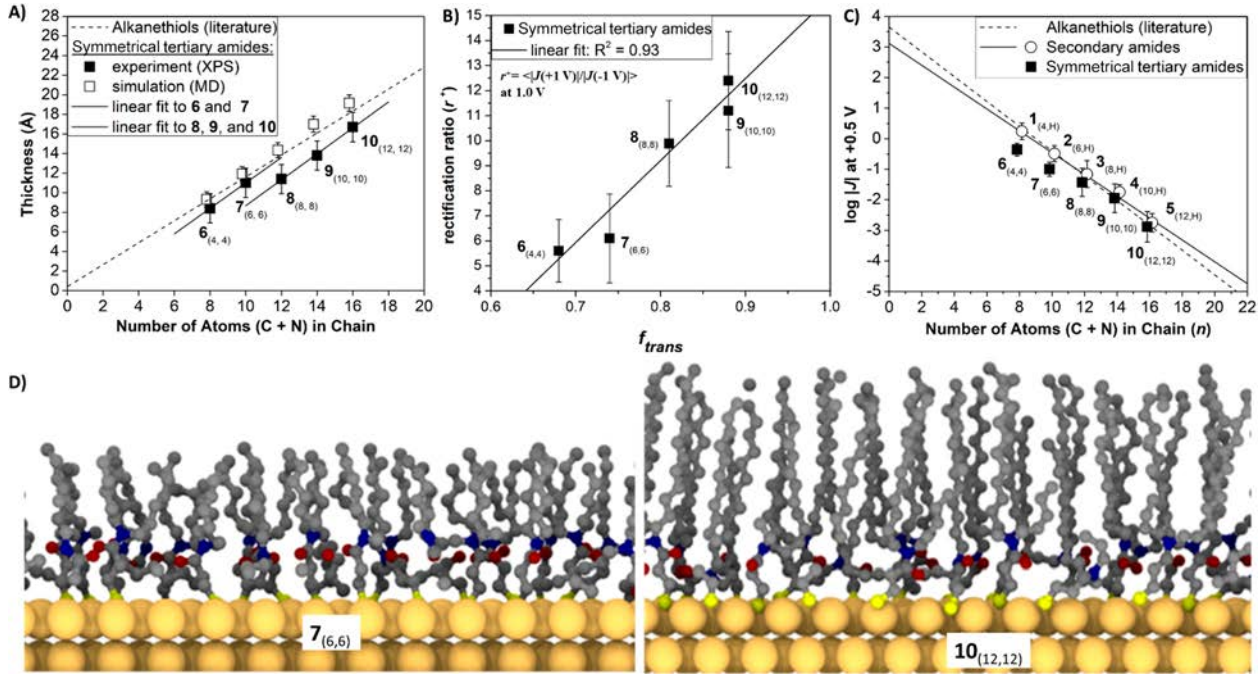

Figure 5. (A) Plot of the measured (filled squares) and simulated (empty squares) thicknesses of SAMs made from symmetrical tertiary amides **6**–**10** (Figure 2), as a function of their chain length. The dashed line represents the corresponding data (from the literature[80]) for alkanethiols. (B) Plot of rectification ratios (r^+) measured at 1.0 V as a function of the conformational order (defined by f_{trans}) of the SAM. (C) Tunneling rates measured for the symmetrical tertiary amides, as a function of their chain length, with the measured rates of secondary amides for comparison. (D) Selected snapshots from the MD simulations of SAMs **2** and **5** (1.5 nm cross sections), depicting their thickness and conformation. Hydrogen atoms have been removed for clarity.

Details), f_{trans} (the fraction of C−C−C−C dihedral angles that are *trans*-extended) and f_{down} (the fraction of alkyl chains that are oriented downward), to represent the conformational order (and disorder) of the molecules making up each SAM.

Secondary Amides Are Well-Ordered and Behave Like Alkanethiols. Our analysis of secondary amides supports previous assertions[44,46] that this class of thiols forms well-ordered SAMs that have packing densities, conformational structures (i.e, *trans*-extended geometries), and tunneling characteristics similar to those of alkanethiols. Figure 4A shows a linear correlation between the thickness (determined by ARXPS) of amides **1**−**5** and the chain length of the molecules (including the amide group), which suggests that these SAMs are well-ordered. The surface coverages (determined by XPS) were nearly indistinguishable from those of alkanethiols (between 0.9×10^{-9} and 1.0×10^{-9} mol/cm^2; see Table S2 in the Supporting Information). This correlation also supports the assertion that these SAMs are well-ordered. The MD simulations, in agreement with the ARXPS results, indicated that the thicknesses of SAMs **1**−**5** increase monotonically with chain length (Figure 4A). These simulations also revealed that their conformations are predominantly *trans* extended ($f_{trans} > 85$) and are all oriented perpendicular to the Au^{TS} surface (i.e., $f_{down} = 0$) (see Table S14 in the Supporting Information for the full list of values of f_{trans} and f_{down}). The value of f_{trans} increased with increasing chain length, which correlates with the well-known transition in alkanethiol SAMs from a more liquid-like (disordered) state to a more crystalline-like (ordered) state, as the chain length increases.[50]

All of the linear amides rectified current at an applied bias of 1.0 V ($r^+ > 5$), possibly because of the proximity and direction of the embedded dipole (from the amide group) to the bottom (Au) electrode.[34] In this work, our investigation of tunneling rates used $J(V)$ at +0.5 V, to avoid complications associated with rectification, which in these molecules takes place only above ∼0.6 V (in the Fowler−Nordheim (F-N) tunneling regime).[34] We observed that the rectification ratio (r^+) was larger in SAMs with longer chain lengths, presumably because the net dipole perpendicular to the mean plane of the metal surface (which seems, in this series, to determine rectification[34]) is larger when the SAMs are more crystalline-like in comparison to that when the SAMs are more liquid-like. This assertion is supported by an approximately linear relationship between the measured rectification (r^+) and f_{trans} shown in Figure 4B. This observation was important, because it suggested that we might be able to use rectification as an indirect experimental metric to compare to the conformational order calculated from the MD simulations.

The measured current densities (log |*J*|) for the linear amides (on a Au^{TS} surface, at an applied bias of +0.5 V) show that the rate of tunneling decreases exponentially with increasing chain length, as it does with alkanethiols (Figure 4C). Within the limits of our measurement, introducing an amide bond at the third carbon from the sulfur atom (*i.e.*, S-$(CH_2)_2$-CONH-R) does not significantly change (relative to those data obtained with alkanethiols) the value of β ($\beta = 0.87 \pm 0.03$) or the value of log $|J_0|$ (log $|J_0| = 3.0 \pm 0.3$).[80] Alkanethiols containing amide groups have previously been shown to have no significant effect on the values of log |*J*| measured at +0.5 V, relative to alkanethiols without amide groups,[81] and if amide-containing alkanethiols form SAMs with the same *trans*-extended, linear orientation of the *n*-alkyl group as alkanethiols, the similarity between their β plots is qualitatively expected.

https://dx.doi.org/10.1021/jacs.0c12571
J. Am. Chem. Soc. 2021, 143, 3481−3493

Symmetrical Tertiary Amides. SAMs made from symmetrically branched, tertiary amides (Figure 2) have structures different from those of secondary amides and alkanethiols. The surface coverages measured by XPS (Table S3 in the Supporting Information) for the symmetrical tertiary amides were between 0.74×10^{-9} and 0.84×10^{-9} mol/cm^2, which is ~16−26% lower than those for secondary amides ($(0.90-1.00) \times 10^{-9}$ mol/cm^2; see Table S1 in the Supporting Information). We attribute this difference in packing density to the increased space occupied by the additional (branching) alkane chain. Figure 5A shows that, for symmetrical tertiary amides **6**−**10** (where $R^1 = R^2$), the thickness of the SAM increases with increasing chain length. This relationship, however, is not entirely linear (as is observed for linear amides or alkanethiols): that is, Figure 5A shows a slight discontinuity between $\mathbf{7}_{(6,6)}$ and $\mathbf{8}_{(8,8)}$. We hypothesize that this divergence from linearity may be a consequence of the transition from SAMs that are liquid crystalline like, to more crystalline like between compounds $\mathbf{7}_{(6,6)}$ and $\mathbf{8}_{(8,8)}$—when the enthalpy (dominated by intermolecular van der Waals forces) begins to overcome the entropy of the system.[50]

The MD simulations of symmetrically branched amides reveal that, as in the case for linear amides, the values of f_{trans} increase with the length of the alkyl chain (Table S14 in the Supporting Information). The same trend is observed for the rectification ratio at 1.0 V (Table S8 in the Supporting Information), which is also larger for symmetrical tertiary amides with longer chain lengths. Figure 5B shows a positive correlation between r^+ and f_{trans}, further supporting the relationship among conformational order, chain length (i.e., SAM crystallinity), and rectification ratio. The values of f_{trans} for the symmetrically branched amides (between 0.70 and 0.88, Table S14 in the Supporting Information) are lower than those for linear amides (0.87−0.99, Table S14 in the Supporting Information). We attribute the increase in *gauche* conformations to the geometrical constraints imposed by the tertiary amide, which prevents an all-*trans* conformation and forces the alkyl chains to adopt a "kink" in their geometry after the point of branching. We note that symmetrical tertiary amides have smaller values of f_{trans} in comparison to linear amides but have comparable values of r^+ (see plots in Figures 4B and 5B). Our interpretation of this result is that r^+ is only indirectly correlated with conformational disorder and that f_{trans} is an indirect (and imperfect) metric for disorder. Thus, while these two metrics are correlated, the absolute value of f_{trans} (derived from simulation) does not determine the absolute value of r^+. In addition to a decrease in f_{trans}, relative to secondary amides, symmetrical tertiary amides have values of $f_{down} > 0$ (Table S14 in the Supporting Information), suggesting that there is significantly more conformational disorder in SAMs formed from symmetrical tertiary amides in comparison to SAMs formed from linear amides. Moreover, the same trend is observed for f_{down} as was observed for f_{trans}: that is, symmetrical tertiary amides with longer chain lengths have more conformational order in comparison to those with shorter chain lengths.

Figure 5C shows that the rate of CT through symmetrical tertiary amides decreases exponentially as a function of chain length, in a manner similar to that observed with alkanethiols and secondary amides.[76] A direct comparison between symmetric tertiary amides and secondary amides with equivalent chain lengths, however, indicates that the rate of CT through symmetrical tertiary amides is lower than that through secondary amides. For instance, the rate of CT in $\mathbf{6}_{(4,4)}$ is 6.3 times lower than that through $\mathbf{1}_{(4,H)}$, despite having the same thickness (measured by ARXPS) and the same chain length. Likewise, CT through $\mathbf{7}_{(6,6)}$ is 2.6 times lower than that through $\mathbf{2}_{(6,H)}$, which has the same chain length and thickness (determined by XPS). The rate of tunneling is also lower through these symmetrical tertiary amides than that through secondary amides when log $|J(V)|$ is plotted as a function of the ARXPS measured monolayer thickness (Figure 6), suggesting

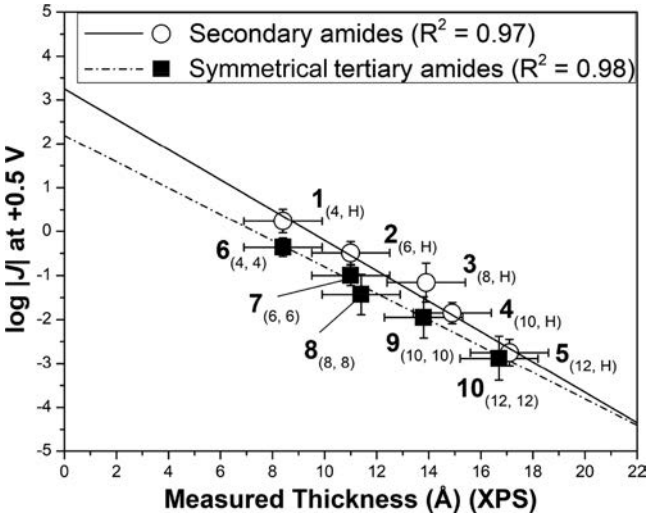

Figure 6. Tunneling rates measured for the linear amides (empty circles) and symmetrically branched amides (solid squares) as a function of their experimentally determined (by XPS) monolayer thickness.

that tunneling rates through tertiary amides are lower than those through secondary amides of equivalent chain length, even when they form monolayers of equivalent (or smaller) thickness.

By excluding a variation in thickness and packing density as the origin of this difference in rate of tunneling between secondary and symmetrical tertiary amides, we conclude—by elimination—that differences in conformation influence the rates of charge tunneling. Because the differences in conformation between secondary amides and symmetrical tertiary amides is a combination of *gauche* defects (defined by f_{trans}) and different chain orientations (defined by f_{down}), we conclude that charge tunneling is more rapid through alkyl chains with *trans*-extended geometries in comparison to those with *gauche* defects and assert that, in these systems, the conformation *does* influence the rate of charge tunneling. This conclusion is consistent with previous measurements of temperature-dependent electrical transport through linear alkyl monolayers on silicon surfaces, where an inverse relationship between tunneling rate and temperature was attributed to cooling-induced ordering of the monolayer (and thus increased intramolecular electronic coupling) on the basis of vibrational and photoelectron spectroscopy.[82]

Series I Amides (Figure 2; $\mathbf{X}_{(n,m)}$, $n + m = 12$). The set of amides in series I was designed to test whether the total number of carbons (regardless of their position in the chain or the conformation of individual bonds) determines the rate of tunneling. This series includes the secondary amide $\mathbf{5}_{(12,H)}$ and the symmetrical tertiary amide $\mathbf{7}_{(6,6)}$. In principle, tunneling might be determined (regardless of mechanism) by the sum of

https://dx.doi.org/10.1021/jacs.0c12571
J. Am. Chem. Soc. 2021, 143, 3481−3493

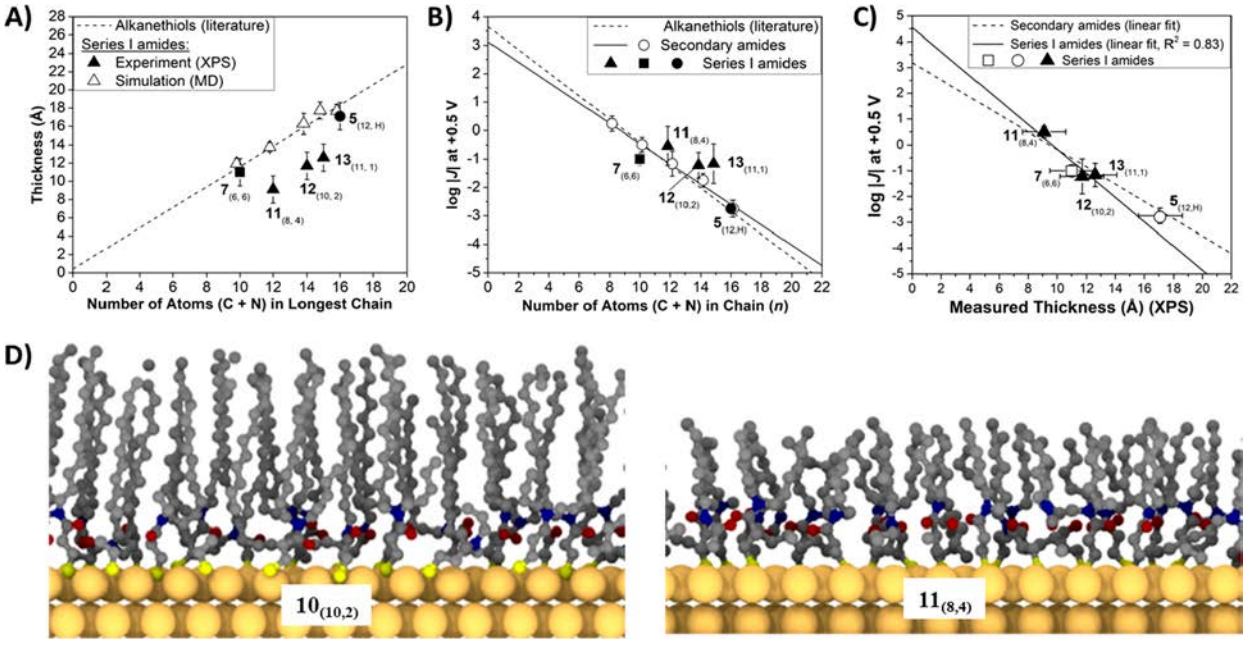

Figure 7. (A) Plot of the measured (filled triangles) and simulated (empty triangles) thicknesses of SAMs made from asymmetrically branched amides **5**, **7**, and **11**−**13**, as a function of their longest chain length. The dashed line represents the corresponding data (from the literature[80]) for alkanethiols. (B) Tunneling rates measured for the asymmetrically branched amides (disordered series I) as a function of their chain length, with the measured rates of linear amides for comparison. (C) Tunneling rates measured for the asymmetrically branched amides (disordered series I) as a function of their measured thickness. (D) Selected snapshots from the MD simulated SAMs (1.5 nm cross sections), depicting their thickness and conformation. Hydrogen atoms have been removed for clarity.

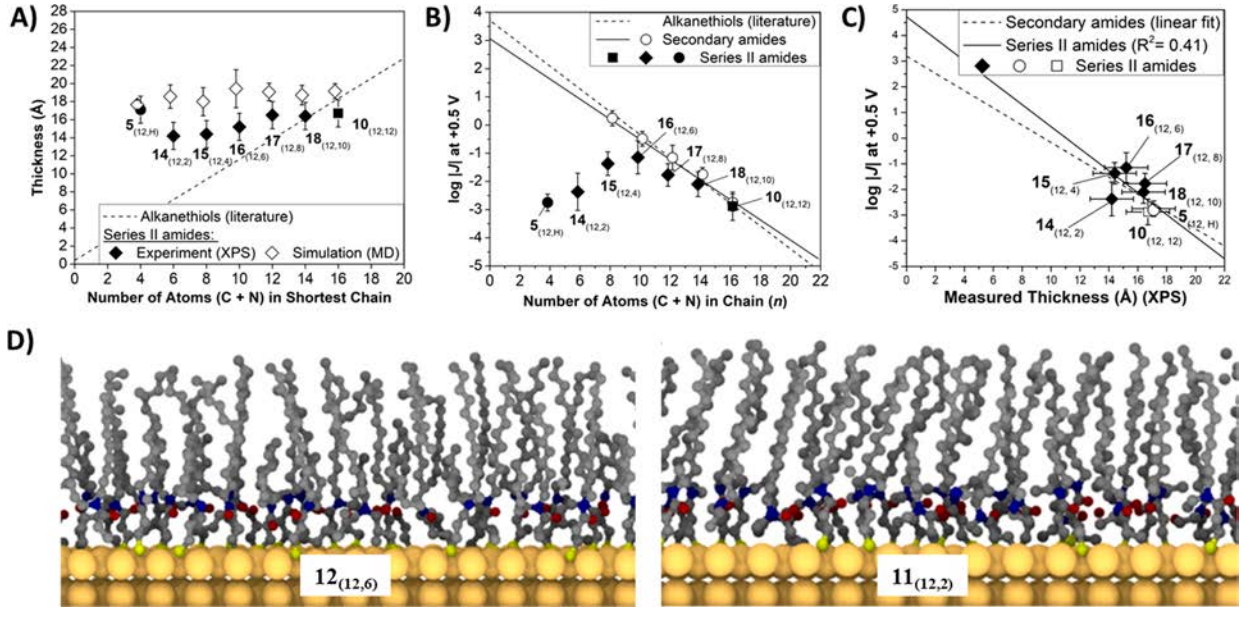

Figure 8. (A) Plot of the measured (filled diamonds) and simulated (empty diamonds) thicknesses of SAMs made from asymmetrically branched amides **5**, **10**, and **14**−**18**, as a function of their longest chain length. (B) Tunneling rates measured for the asymmetrically branched amides (disordered series II) as a function of their chain length, with the measured rates of linear amides for comparison. (C) Tunneling rates measured for the asymmetrically branched amides (disordered series II) as a function of their measured thickness. (D) Selected snapshots from the MD simulated SAMs (1.5 nm cross sections), depicting their thickness and conformation. Hydrogen atoms have been removed for clarity.

the carbon atoms in the monolayer per unit area. Our results (Figure 7B), however, show that asymmetry in branching within SAMs—not just the total number of carbon atoms—leads to differences in tunneling rates, despite the fact that the SAMs have the same number and type of atoms per unit area.

ARXPS measurements indicated that the asymmetrical tertiary amides within series I (i.e., **11**$_{(8,4)}$, **12**$_{(10,2)}$, and **13**$_{(11,1)}$) had lower packing densities in comparison to secondary amides but larger packing densities in comparison to symmetrical tertiary amides. The thickness (measured by ARXPS) of these asymmetrical tertiary amides increased as the length of chain *a* increased, suggesting that the longest chain length dominates the thickness of these SAMs.

https://dx.doi.org/10.1021/jacs.0c12571
J. Am. Chem. Soc. 2021, 143, 3481−3493

Our simulations suggest that, like the symmetrical tertiary amides, the presence of a second alkyl chain causes a kink in the conformation, which leads to more *gauche* conformations than in linear amides (Table S14 in the Supporting Information). In agreement with the observed trends in rectification ratios, all of the asymmetrically branched amides had $r^+ < 7.0$. This result indicated that the amides are less ordered in their orientation with respect to the surface of the gold in comparison to linear amides and thus that these SAMs of tertiary amides are probably in more disordered conformations. This conclusion was supported by our MD simulations, particularly for SAMs made from amide $\mathbf{11}_{(8,4)}$ ($f_{trans} = 0.78, f_{down} = 0.58$) and SAMs made from amide $\mathbf{12}_{(10,2)}$ ($f_{trans} = 0.91$, $f_{down} = 0.35$), which indicate substantial conformational disorder.

Unlike the secondary amides and symmetrical tertiary amides, the current density measurements for series I amides did not correlate linearly with chain length (Figure 7A, $R^2 = 0.65$). A positive correlation was observed, however, between the current density and the thickness (determined by ARXPS) of the SAMs (Figure 7C, $R^2 = 0.83$). While this result implies that the rate of tunneling through this set of SAMs—even when they have disordered conformations—still correlates with the thickness of the monolayer, the value of β (i.e., the slope) is larger for series I amides than for secondary amides. This difference in β indicates that the relationship between thickness and $J(V)$ may be different for ordered than for disordered SAMs.

Series II Amides (Figure 2; $\mathbf{X}_{(n,m)}$, $n = 12$). Series II amides, which include the asymmetrical tertiary amides **14**–**18**, the secondary amide $\mathbf{5}_{(12,H)}$ and the symmetrical tertiary amide $\mathbf{10}_{(12,12)}$, was designed to test how the asymmetry in branching (which we believe correlates with conformational disorder) influences tunneling. Measurements of packing density by XPS indicated that, like series I amides, the density of asymmetrical tertiary amides (i.e., **14**–**18**) was greater than that of symmetrical tertiary amides but less than that of secondary amides. This result suggests that asymmetrical branching forces the longer chain to adopt a bent conformation, in order to maximize their intermolecular contacts and reduce the volume they occupy on the surface. The thickness of the monolayers (as measured by ARXPS) across the series remained approximately the same (Figure 8A), comparable to the case for the linear amide $\mathbf{5}_{(12,H)}$. A small decrease in thickness was observed as the length of chain *b* decreased, but chain *a*—with its greater number of carbon atoms—appeared to dominate the thickness of the monolayer. The simulations also show a relatively constant thickness of the monolayer for this series of amides (Figure 8A).

The rectification ratios at 1.0 V for amides ($r^+ < 7.5$; Table S12 in the Supporting Information) are all lower than those for the well-ordered SAMs in the series, $\mathbf{5}_{(12,H)}$ ($r^+ = 10.42$) and $\mathbf{10}_{(12,12)}$ ($r^+ = 11.22$), which suggests that amides **14**–**18** form disordered SAMs. This interpretation was supported by the MD simulations (Table S14 in the Supporting Information), which show a significant number of *gauche* conformations (f_{trans} ranges from 0.82 to 0.93) and varied chain orientations (f_{down} ranges from 0.15 to 0.6).

The tunneling rates of series II amides (Figure 8B) are all higher than that of a corresponding secondary amide of length $n = 16$ (i.e, $\mathbf{5}_{(12,H)}$). From the results of series I amides, however, we did not expect that the rates of tunneling would necessarily correlate with chain length, and we thus plotted log $|J(V)|$ against monolayer thickness in Figure 8C. Unlike the case with series I amides, we observed no linear relationship between log $|J(V)|$ and monolayer thickness for series II amides, indicating that in this series the rate of charge tunneling does not correlate directly with thickness. Moreover, the discrepancy between $J(V)$ and thickness of **14**–**18**, relative to $\mathbf{10}_{(12,12)}$ or $\mathbf{5}_{(12,H)}$, cannot be accounted for by changes in packing density within the SAM (as **5** has a higher packing density than any of **14**–**18** and **10** has a lower packing density than any of **14**–**18**). We thus conclude, again by elimination, that the conformation of these SAMs must be influencing the rate of tunneling and that conformation *does* influence tunneling rates in molecular junctions.

Unlike symmetrical tertiary amides, the unsymmetrical tertiary amides in series II have tunneling rates that are higher than those of secondary amides (or alkanethiols) of equivalent thickness (or chain length). We believe that this result is a consequence of the asymmetry in the lengths of chains *a* and *b*, which causes more extensive disorder in asymmetrical tertiary amides than in symmetric tertiary amides. This difference in disorder could result in a poorly defined interface between the top EGaIn electrode and the SAM and may cause electrical contacts to be made farther down the chain than the ARXPS-determined thickness would suggest.

CONCLUSION

By analyzing molecules that are similar electronically but that differ in their conformation, we studied the effects of conformation, thickness, and packing density of molecules in a SAM on the rate of charge transport (CT) through them. We observe differences in tunneling characteristics that cannot be accounted for by changes in thickness or packing density and conclude by elimination that charge tunneling through SAMs *is* influenced by the conformations of the molecules and is not solely determined by the distance between the two electrodes.

By comparing symmetric tertiary amides to secondary amides, we conclude that the rate of CT is higher through alkane chains with *trans* conformations than through those with *gauche* conformations. By analyzing Series I amides, which have the same number and type of atoms but are distributed differently among chains *a* and *b*, we conclude that the spatial arrangement of atoms matters. That is, tunneling is not solely dependent on the density of atoms of a particular type within the monolayer. These results suggest that CT may be a through-bond process.

We conclude from our analysis of series II amides that the conformation (or conformational disorder) influences the rates of CT. This series revealed that a change in thickness does not always correlate with an equivalent change in $J(V)$, even for simple alkanethiols. We believe that the results of this series of amides indicate that conformational disorder can create a poorly defined electrode–molecule interface, which can artificially increase $J(V)$.

Finally, we observed a clear relationship between conformational order and the dipole-induced rectification in these systems. Specifically, SAMs that were more conformationally ordered yielded molecular junctions with larger rectification ratios in comparison to more conformationally disordered SAMs. This result strongly suggests that conformation, and not solely molecular structure, should be considered in the design and analysis of molecular junctions.

https://dx.doi.org/10.1021/jacs.0c12571
J. Am. Chem. Soc. 2021, 143, 3481–3493

■ ASSOCIATED CONTENT

Supporting Information

The Supporting Information is available free of charge at https://pubs.acs.org/doi/10.1021/jacs.0c12571.

Materials, junction measurements using "selected" conical tips of EGaIn, EGaIn measurement protocol, angular-dependent X-ray photoelectron spectroscopy, computational methods, comparison between experimental and simulated monolayer thickness, summary of XPS data, summary of tunneling data, summary of simulation data, syntheses, and contact angle data (PDF)

■ AUTHOR INFORMATION

Corresponding Author

George M. Whitesides − *Department of Chemistry and Chemical Biology, Harvard University, Cambridge, Massachusetts 02138, United States;* orcid.org/0000-0001-9451-2442; Email: gwhitesides@gmwgroup.harvard.edu

Authors

Lee Belding − *Department of Chemistry and Chemical Biology, Harvard University, Cambridge, Massachusetts 02138, United States*

Samuel E. Root − *Department of Chemistry and Chemical Biology, Harvard University, Cambridge, Massachusetts 02138, United States*

Yuan Li − *Department of Chemistry and Chemical Biology, Harvard University, Cambridge, Massachusetts 02138, United States*

Junwoo Park − *Department of Chemistry and Chemical Biology, Harvard University, Cambridge, Massachusetts 02138, United States*

Mostafa Baghbanzadeh − *Department of Chemistry and Chemical Biology, Harvard University, Cambridge, Massachusetts 02138, United States;* orcid.org/0000-0001-7678-1681

Edwin Rojas − *Department of Chemistry and Chemical Biology, Harvard University, Cambridge, Massachusetts 02138, United States*

Priscilla F. Pieters − *Department of Chemistry and Chemical Biology, Harvard University, Cambridge, Massachusetts 02138, United States*

Hyo Jae Yoon − *Department of Chemistry, Korea University, Seoul 02841, Korea*

Complete contact information is available at: https://pubs.acs.org/10.1021/jacs.0c12571

Author Contributions

[§]L.B. and S.E.R. contributed equally.

Notes

The authors declare no competing financial interest.

■ ACKNOWLEDGMENTS

This work was supported by NSF award CHE-1808361. L.B. acknowledges fellowship support from NSERC Canada. E.R. acknowledges the Harvard REU program under NSF award DMR-1420570. Sample characterization was performed in part at the Center for Nanoscale Systems (CNS) at Harvard University, a member of the National Nanotechnology Infrastructure Network (NNIN), which is supported by the National Science Foundation (ECS-0335765). This work used the Extreme Science and Engineering Discovery Environment (XSEDE) Comet supercomputer at the San Diego Supercomputer Center through allocation DMR180105, which is supported by National Science Foundation grant number ACI-1548562.[83] H.J.Y. acknowledges support from the NRF of Korea (NRF-2019R1A2C2011003, NRF-2019R1A6A1A11044070) and the Future Research Grant (FRG) of Korea University.

■ REFERENCES

(1) Venkataraman, L.; Klare, J. E.; Nuckolls, C.; Hybertsen, M. S.; Steigerwald, M. L. Dependence of single-molecule junction conductance on molecular conformation. *Nature* **2006**, *442*, 904−907.

(2) Kong, G. D.; Jin, J.; Thuo, M.; Song, H.; Joung, J. F.; Park, S.; Yoon, H. J. Elucidating the role of molecule−electrode interfacial defects in charge tunneling characteristics of large-area junctions. *J. Am. Chem. Soc.* **2018**, *140*, 12303−12307.

(3) Kong, G. D.; Byeon, S. E.; Park, S.; Song, H.; Kim, S.-Y.; Yoon, H. J. Mixed molecular electronics: tunneling behaviors and applications of mixed self-assembled monolayers. *Adv. Electron. Mater.* **2020**, *6*, 1901157−1901176.

(4) Chen, J.; Chang, B.; Oyola-Reynoso, S.; Wang, Z.; Thuo, M. Quantifying gauche defects and phase evolution in self-assembled monolayers through sessile drops. *ACS Omega* **2017**, *2*, 2072−2084.

(5) Justeena, A. N.; Nirmal, D.; Gracia, D. In Design and analysis of tunnel FET using high K dielectric materials. *International Conference on Innovations in Electrical, Electronics, Instrumentation and Media Technology (ICEEIMT)* **2017**, *2017*, 177.

(6) Anghel, C.; Chilagani, P.; Amara, A.; Vladimirescu, A. Tunnel field effect transistor with increased ON current, low-k spacer and high-k dielectric. *Appl. Phys. Lett.* **2010**, *96*, 122104−122104−3.

(7) Editorial. Molecular electronics under the microscope. *Nat. Chem.* **2015**, *7*, 181.

(8) Martínez Hardigree, J. F.; Dawidczyk, T. J.; Ireland, R. M.; Johns, G. L.; Jung, B.-J.; Nyman, M.; Österbacka, R.; Marković, N.; Katz, H. E. Reducing leakage currents in n-channel organic field-effect transistors using molecular dipole monolayers on nanoscale oxides. *ACS Appl. Mater. Interfaces* **2013**, *5*, 7025−7032.

(9) Klauk, H.; Zschieschang, U.; Pflaum, J.; Halik, M. Ultralow-power organic complementary circuits. *Nature* **2007**, *445*, 745.

(10) Szent-Györgyi, A. Towards a new biochemistry? *Science* **1941**, *93*, 609−611.

(11) Gray, H. B.; Halpern, J. Distant charge transport. *Proc. Natl. Acad. Sci. U. S. A.* **2005**, *102*, 3533−3534.

(12) Boal, A. K.; Yavin, E.; Lukianova, O. A.; O'Shea, V. L.; David, S. S.; Barton, J. K. DNA-Bound Redox Activity of DNA Repair Glycosylases Containing [4Fe-4S] Clusters. *Biochemistry* **2005**, *44*, 8397−8407.

(13) Yavin, E.; Boal, A. K.; Stemp, E. D. A.; Boon, E. M.; Livingston, A. L.; Shea, V. L.; David, S. S.; Barton, J. K. Protein−DNA charge transport: Redox activation of a DNA repair protein by guanine radical. *Proc. Natl. Acad. Sci. U. S. A.* **2005**, *102*, 3546−3551.

(14) Sjulstok, E.; Olsen, J. M. H.; Solov'yov, I. A. Quantifying electron transfer reactions in biological systems: what interactions play the major role? *Sci. Rep.* **2016**, *5*, 18446−18457.

(15) Bothe, H.; Schmitz, O.; Yates, M. G.; Newton, W. E. Nitrogen fixation and hydrogen metabolism in cyanobacteria. *Microbiol. Mol. Biol. Rev.* **2010**, *74*, 529−551.

(16) Mishchenko, A.; Vonlanthen, D.; Meded, V.; Bürkle, M.; Li, C.; Pobelov, I. V.; Bagrets, A.; Viljas, J. K.; Pauly, F.; Evers, F.; Mayor, M.; Wandlowski, T. Influence of conformation on conductance of biphenyl-dithiol single-molecule contacts. *Nano Lett.* **2010**, *10*, 156−163.

(17) Xie, Z.; Bâldea, I.; Frisbie, C. D. Determination of energy-level alignment in molecular tunnel junctions by transport and spectroscopy: self-consistency for the case of oligophenylene thiols and

dithiols on Ag, Au, and Pt electrodes. *J. Am. Chem. Soc.* **2019**, *141*, 3670−3681.
(18) Li, G.; Xie, J.; Wang, J.; Xia, L.; Li, Y.; Hu, W. Nanoscale surface disorder for enhanced solar absorption and superior visible-light photocatalytic property in Ti-rich BaTiO3 nanocrystals. *ACS Omega* **2019**, *4*, 9673−9679.
(19) Haberhauer, G.; Gleiter, R.; Burkhart, C. Planarized Intramolecular Charge Transfer: A Concept for Fluorophores with both Large Stokes Shifts and High Fluorescence Quantum Yields. *Chem. - Eur. J.* **2016**, *22*, 971−978.
(20) Belding, L.; Guest, M.; Le Sueur, R.; Dudding, T. Fluorescence of Cyclopropenium Ion Derivatives. *J. Org. Chem.* **2018**, *83*, 6489−6497.
(21) Nikitina, V. A.; Rudnev, A. V.; Nazmutdinov, R. R.; Tsirlina, G. A.; Wandlowski, T. Solvent effect on electron transfer through alkanethiols. *J. Elect. Chem.* **2018**, *819*, 58−64.
(22) Juárez, E. G.; Mena-Cervantes, V. Y.; Vazquez-Arenas, J.; Flores, G. P.; Hernandez-Altamirano, R. Inhibition of CO_2 corrosion via sustainable geminal zwitterionic compounds: effect of the length of the hydrocarbon chain from amines. *ACS Sustainable Chem. Eng.* **2018**, *6*, 17230−17238.
(23) Vilan, A.; Aswal, D.; Cahen, D. Large-area, ensemble molecular electronics: motivation and challenges. *Chem. Rev.* **2017**, *117*, 4248−4286.
(24) Liu, D.; Miao, Q. Recent progress in interface engineering of organic thin film transistors with self-assembled monolayers. *Mater. Chem. Front.* **2018**, *2*, 11−21.
(25) Love, J. C.; Estroff, L. A.; Kriebel, J. K.; Nuzzo, R. G.; Whitesides, G. M. Self-assembled monolayers of thiolates on metals as a form of nanotechnology. *Chem. Rev.* **2005**, *105*, 1103−1170.
(26) Jeong, H.; Kim, D.; Xiang, D.; Lee, T. High-yield functional molecular electronic devices. *ACS Nano* **2017**, *11*, 6511−6548.
(27) Lindsey, J. S.; Bocian, D. F. Molecules for charge-based information storage. *Acc. Chem. Res.* **2011**, *44*, 638−650.
(28) Beebe, J. M.; Engelkes, V. B.; Miller, L. L.; Frisbie, C. D. Contact resistance in metal−molecule−metal junctions based on aliphatic sams: effects of surface linker and metal work function. *J. Am. Chem. Soc.* **2002**, *124*, 11268−11269.
(29) Bowers, C. M.; Liao, K.-C.; Yoon, H. J.; Rappoport, D.; Baghbanzadeh, M.; Simeone, F. C.; Whitesides, G. M. Introducing ionic and/or hydrogen bonds into the SAM//Ga_2O_3 top-interface of $Ag^{TS}/S(CH_2)_nT//Ga_2O_3$/EGaIn junctions. *Nano Lett.* **2014**, *14*, 3521−3526.
(30) Liao, K.-C.; Yoon, H. J.; Bowers, C. M.; Simeone, F. C.; Whitesides, G. M. Replacing $Ag^{TS}SCH_2$-R with $Ag^{TS}O_2C$-R in EGaIn-based tunneling junctions does not significantly change rates of charge transport. *Angew. Chem., Int. Ed.* **2014**, *53*, 3889−3893.
(31) Yoon, H. J.; Shapiro, N. D.; Park, K. M.; Thuo, M. M.; Soh, S.; Whitesides, G. M. The rate of charge tunneling through self-assembled monolayers is insensitive to many functional group substitutions. *Angew. Chem., Int. Ed.* **2012**, *51*, 4658−4661.
(32) Cafferty, B. J.; Yuan, L.; Baghbanzadeh, M.; Rappoport, D.; Beyzavi, M. H.; Whitesides, G. M. Charge transport through self-assembled monolayers of monoterpenoids. *Angew. Chem., Int. Ed.* **2019**, *58*, 8097−8102.
(33) Yoon, H. J.; Shapiro, N. D.; Park, K. M.; Thuo, M. M.; Soh, S.; Whitesides, G. M. The rate of charge tunneling through self-assembled monolayers is insensitive to many functional group substitutions. *Angew. Chem., Int. Ed.* **2012**, *51*, 4658−4661.
(34) Baghbanzadeh, M.; Belding, L.; Yuan, L.; Park, J.; Al-Sayah, M. H.; Bowers, C. M.; Whitesides, G. M. Dipole-induced rectification across Ag^{TS}/SAM//Ga_2O_3/EGaIn junctions. *J. Am. Chem. Soc.* **2019**, *141*, 8969−8980.
(35) Lenfant, S.; Krzeminski, C.; Delerue, C.; Allan, G.; Vuillaume, D. Molecular rectifying diodes from self-assembly on silicon. *Nano Lett.* **2003**, *3*, 741−746.
(36) Yoon, H. J.; Liao, K.-C.; Lockett, M. R.; Kwok, S. W.; Baghbanzadeh, M.; Whitesides, G. M. Rectification in tunneling junctions: 2,2′-bipyridyl-terminated n-alkanethiolates. *J. Am. Chem. Soc.* **2014**, *136*, 17155−17162.
(37) Nijhuis, C. A.; Reus, W. F.; Whitesides, G. M. Mechanism of rectification in tunneling junctions based on molecules with asymmetric potential drops. *J. Am. Chem. Soc.* **2010**, *132*, 18386−18401.
(38) Cho, S. J.; Kong, G. D.; Park, S.; Park, J.; Byeon, S. E.; Kim, T.; Yoon, H. J. Molecularly controlled stark effect induces significant rectification in polycyclic-aromatic-hydrocarbon-terminated n-alkanethiolates. *Nano Lett.* **2019**, *19*, 545−553.
(39) Hegner, M.; Wagner, P.; Semenza, G. Ultralarge atomically flat template-stripped Au surfaces for scanning probe microscopy. *Surf. Sci.* **1993**, *291*, 39−46.
(40) Jiang, L.; Sangeeth, C. S. S.; Yuan, L.; Thompson, D.; Nijhuis, C. A. One-nanometer thin monolayers remove the deleterious effect of substrate defects in molecular tunnel junctions. *Nano Lett.* **2015**, *15*, 6643−6649.
(41) Novak, M.; Jäger, C. M.; Rumpel, A.; Kropp, H.; Peukert, W.; Clark, T.; Halik, M. The morphology of integrated self-assembled monolayers and their impact on devices − A computational and experimental approach. *Org. Electron.* **2010**, *11*, 1476.
(42) Levine, I.; Weber, S. M.; Feldman, Y.; Bendikov, T.; Cohen, H.; Cahen, D.; Vilan, A. Molecular Length, Monolayer Density, and Charge Transport: Lessons from Al−AlOx/Alkyl−Phosphonate/Hg Junctions. *Langmuir* **2012**, *28*, 404.
(43) Nishi, N.; Hobara, D.; Yamamoto, M.; Kakiuchi, T. Chain-length-dependent change in the structure of self-assembled monolayers of n-alkanethiols on Au(111) probed by broad-bandwidth sum frequency generation spectroscopy. *J. Chem. Phys.* **2003**, *118*, 1904−1911.
(44) Lewis, P. A.; Smith, R. K.; Kelly, K. F.; Bumm, L. A.; Reed, S. M.; Clegg, R. S.; Gunderson, J. D.; Hutchison, J. E.; Weiss, P. S. The Role of Buried Hydrogen Bonds in Self-Assembled Mixed Composition Thiols on Au{111}. *J. Phys. Chem. B* **2001**, *105*, 10630−10636.
(45) Smith, R. K.; Reed, S. M.; Lewis, P. A.; Monnell, J. D.; Clegg, R. S.; Kelly, K. F.; Bumm, L. A.; Hutchison, J. E.; Weiss, P. S. Phase separation within a binary self-assembled monolayer on Au{111} driven by an amide-containing alkanethiol. *J. Phys. Chem. B* **2001**, *105*, 1119−1122.
(46) Thomas, J. C.; Goronzy, D. P.; Dragomiretskiy, K.; Zosso, D.; Gilles, J.; Osher, S. J.; Bertozzi, A. L.; Weiss, P. S. Mapping buried hydrogen-bonding networks. *ACS Nano* **2016**, *10*, 5446−5451.
(47) Sek, S.; Palys, B.; Bilewicz, R. Contribution of intermolecular interactions to electron transfer through monolayers of alkanethiols containing amide groups. *J. Phys. Chem. B* **2002**, *106*, 5907−5914.
(48) Angelova, P. N.; Hinrichs, K.; Philipova, I. L.; Kostova, K. V.; Tsankov, D. T. Monolayer orientation of ω-substituted amide-bridged alkanethiols on gold. *J. Phys. Chem. C* **2010**, *114*, 1253−1259.
(49) Clegg, R. S.; Hutchison, J. E. Control of Monolayer Assembly Structure by Hydrogen Bonding Rather Than by Adsorbate−Substrate Templating. *J. Am. Chem. Soc.* **1999**, *121*, 5319−5327.
(50) Clegg, R. S.; Reed, S. M.; Smith, R. K.; Barron, B. L.; Rear, J. A.; Hutchison, J. E. The interplay of lateral and tiered interactions in stratified self-organized molecular assemblies. *Langmuir* **1999**, *15*, 8876−8883.
(51) Shon, Y.-S.; Lee, T. R. Chelating self-assembled monolayers on gold generated from spiroalkanedithiols. *Langmuir* **1999**, *15*, 1136−1140.
(52) Shon, Y.-S.; Lee, S.; Perry, S. S.; Lee, T. R. The adsorption of unsymmetrical spiroalkanedithiols onto gold affords multi-component interfaces that are homogeneously mixed at the molecular level. *J. Am. Chem. Soc.* **2000**, *122*, 1278−1283.
(53) Park, J.-S.; Smith, A. C.; Lee, T. R. Loosely packed self-assembled monolayers on gold generated from 2-Alkyl-2-methyl-propane-1,3-dithiols. *Langmuir* **2004**, *20*, 5829−5839.
(54) San Juan, R. R.; Carmichael, T. B. Formation of self-assembled monolayers with homogeneously mixed, loosely packed alkyl groups

https://dx.doi.org/10.1021/jacs.0c12571
J. Am. Chem. Soc. 2021, 143, 3481−3493

using unsymmetrical dialkyldithiophosphinic acids. *Langmuir* **2012**, *28*, 17701−17708.
(55) Troughton, E. B.; Bain, C. D.; Whitesides, G. M.; Nuzzo, R. G.; Allara, D. L.; Porter, M. D. Monolayer films prepared by the spontaneous self-assembly of symmetrical and unsymmetrical dialkyl sulfides from solution onto gold substrates: structure, properties, and reactivity of constituent functional groups. *Langmuir* **1988**, *4*, 365−385.
(56) Slowinski, K.; Chamberlain, R. V.; Miller, C. J.; Majda, M. Through-bond and chain-to-chain coupling. two pathways in electron tunneling through liquid alkanethiol monolayers on mercury electrodes. *J. Am. Chem. Soc.* **1997**, *119*, 11910−11919.
(57) Slowinski, K.; Fong, H. K. Y.; Majda, M. Mercury−mercury tunneling junctions. 1. electron tunneling across symmetric and asymmetric alkanethiolate bilayers. *J. Am. Chem. Soc.* **1999**, *121*, 7257−72261.
(58) Beebe, J. M.; Engelkes, V. B.; Liu, J.; Gooding, J. J.; Eggers, P. K.; Jun, Y.; Zhu, X.; Paddon-Row, M. N.; Frisbie, C. D. Length dependence of charge transport in nanoscopic molecular junctions incorporating a series of rigid thiol-terminated norbornylogs. *J. Phys. Chem. B* **2005**, *109*, 5207−5216.
(59) Yang, W. R.; Jones, M. W.; Li, X.; Eggers, P. K.; Tao, N.; Gooding, J. J.; Paddon-Row, M. N. Single molecule conductance through rigid norbornylogous bridges with zero average curvature. *J. Phys. Chem. C* **2008**, *112*, 9072−9080.
(60) Haran, A.; Waldeck, D. H.; Naaman, R.; Moons, E.; Cahen, D. The dependence of electron transfer efficiency on the conformational order in organic monolayers. *Science* **1994**, *263*, 948−950.
(61) Wang, Y.-F.; Yang, G.; Liu, C.-B. Electron transfers in proteins: Investigations with a modified through-bond coupling model. *Phys.Rev. E* **2009**, *80*, 021927−021927−8.
(62) Berstis, L.; Beckham, G. T.; Crowley, M. F. Electronic coupling through natural amino acids. *J. Chem. Phys.* **2015**, *143*, 225102−225102−10.
(63) Salomon, A.; Cahen, D.; Lindsay, S.; Tomfohr, J.; Engelkes, V. B.; Frisbie, C. D. Comparison of electronic transport measurements on organic molecules. *Adv. Mater.* **2003**, *15*, 1881−1890.
(64) Pathak, A.; Bora, A.; Liao, K.-C.; Schmolke, H.; Jung, A.; Klages, C.-P.; Shwartz; Tornow, M. Disorder-derived, strong tunneling attenuation in bis-phosphonate monolayers. *J. Phys.: Condens. Matter* **2016**, *28*, 094008−094020.
(65) Jones, D. R.; Troisi, A. Single molecule conductance of linear dithioalkanes in the liquid phase: apparently activated transport due to conformational flexibility. *J. Phys. Chem. C* **2007**, *111*, 14567−14573.
(66) Salomon, A.; Shpaisman, H.; Seitz, O.; Boecking, T.; Cahen, D. Temperature-dependent electronic transport through alkyl chain monolayers: evidence for a molecular signature. *J. Phys. Chem. C* **2008**, *112*, 3969−3974.
(67) Haiss, W.; van Zalinge, H.; Bethell, D.; Ulstrup, J.; Schiffrin, D. J.; Nichols, R. J. Thermal gating of the single molecule conductance of alkanedithiols. *Faraday Discuss.* **2006**, *131*, 253−264.
(68) Martín, S.; Giustiniano, F.; Haiss, W.; Higgins, S. J.; Whitby, R. J.; Nichols, R. J. Influence of conformational flexibility on single-molecule conductance in nano-electrical junctions. *J. Phys. Chem. C* **2009**, *113*, 18884−18890.
(69) Frederiksen, T.; Munuera, C.; Ocal, C.; Brandbyge, M.; Paulsson, M.; Sanchez-Portal, D.; Arnau, A. Exploring the tilt-angle dependence of electron tunneling across molecular junctions of self-assembled alkanethiols. *ACS Nano* **2009**, *3*, 2073−2080.
(70) Wang, G.; Kim, T.-W.; Jo, G.; Lee, T. Enhancement of field emission transport by molecular tilt configuration in metal−molecule−metal junctions. *J. Am. Chem. Soc.* **2009**, *131*, 5980−5981.
(71) Song, H.; Lee, H.; Lee, T. Intermolecular chain-to-chain tunneling in metal−alkanethiol−metal junctions. *J. Am. Chem. Soc.* **2007**, *129*, 3806−3807.
(72) Yuan, L.; Jiang, L.; Zhang, B.; Nijhuis, C. A. Dependency of the tunneling decay coefficient in molecular tunneling junctions on the topography of the bottom electrodes. *Angew. Chem., Int. Ed.* **2014**, *53*, 3377−3381.
(73) Weiss, E. A.; Chiechi, R. C.; Kaufman, G. K.; Kriebel, J. K.; Li, Z.; Duati, M.; Rampi, M. A.; Whitesides, G. M. Influence of defects on the electrical characteristics of mercury-drop junctions: self-assembled monolayers of n-alkanethiolates on rough and smooth silver. *J. Am. Chem. Soc.* **2007**, *129*, 4336−4349.
(74) Kovalchuk, A.; Abu-Husein, T.; Fracasso, D.; Egger, D. A.; Zojer, E.; Zharnikov, M.; Terfort, A.; Chiechi, R. C. Transition voltages respond to synthetic reorientation of embedded dipoles in self-assembled monolayers. *Chem. Sci.* **2016**, *7*, 781−787.
(75) Banks, J. L.; Beard, H. S.; Cao, Y.; Cho, A. E.; Damm, W.; Farid, R.; Felts, A. K.; Halgren, T. A.; Mainz, D. T.; Maple, J. R.; Murphy, R.; Philipp, D. M.; Repasky, M. P.; Zhang, L. Y.; Berne, B. J.; Friesner, R. A.; Gallicchio, E.; Levy, R. M. Integrated modeling program, applied chemical theory (IMPACT). *J. Comput. Chem.* **2005**, *26*, 1752−1780.
(76) Plimpton, S. Fast parallel algorithms for short-range molecular dynamics. *J. Comput. Phys.* **1995**, *117*, 1−19.
(77) Stukowski, A. Visualization and analysis of atomistic simulation data with OVITO−the Open Visualization Tool. *Modell. Simul. Mater. Sci. Eng.* **2010**, *18*, 015012−015033.
(78) Simeone, F. C.; Yoon, H. J.; Thuo, M. M.; Barber, J. R.; Smith, B.; Whitesides, G. M. Defining the value of injection current and effective electrical contact area for EGaIn-based molecular tunneling junctions. *J. Am. Chem. Soc.* **2013**, *135*, 18131−18144.
(79) Simmons, J. G. Electric tunnel effect between dissimilar electrodes separated by a thin insulating film. *J. Appl. Phys.* **1963**, *34*, 2581−2587.
(80) Baghbanzadeh, M.; Simeone, F. C.; Bowers, C. M.; Liao, K.-C.; Thuo, M.; Baghbanzadeh, M.; Miller, M. S.; Carmichael, T. B.; Whitesides, G. M. Odd−even effects in charge transport across n-alkanethiolate-based SAMs. *J. Am. Chem. Soc.* **2014**, *136*, 16919−16925.
(81) Thuo, M. M.; Reus, W. F.; Simeone, F. C.; Kim, C.; Schulz, M. D.; Yoon, H. J.; Whitesides, G. M. Replacing $-CH_2CH_2-$ with $-CONH-$ does not significantly change rates of charge transport through Ag^{TS}-SAM//Ga_2O_3/EGaIn junctions. *J. Am. Chem. Soc.* **2012**, *134*, 10876−10884.
(82) Shpaisman, H.; Seitz, O.; Yaffe, O.; Roodenko, K.; Scheres, L.; Zuilhof, H.; Chabal, Y. J.; Sueyoshi, T.; Kera, S.; Ueno, N.; Vilan, A.; Cahen, D. Structure Matters: Correlating temperature dependent electrical transport through alkyl monolayers with vibrational and photoelectron spectoscopies. *Chemical Science* **2012**, *3*, 851−862.
(83) Towns, J.; Cockerill, T.; Dahan, M.; Foster, I.; Gaither, K.; Grimshaw, A.; Hazlewood, V.; Lathrop, S.; Lifka, D.; Peterson, G. D.; Roskies, R.; Scott, J. R.; Wilkins-Diehr, N. XSEDE: Accelerating Scientific Discovery. *Comput. Sci. Eng.* **2014**, *16*, 62−74.

https://dx.doi.org/10.1021/jacs.0c12571
J. Am. Chem. Soc. 2021, 143, 3481−3493